*Science, Engineering & Education,8, (1), 2023, 77-85*

# Design, Fabrication and Dynamic Performance Analysis of Magneto-Rheological Damper Suitable for Vehicle Application

Noojaje Purushothama Puneet*, Abhinandan Hegale,
Hemantha Kumar, Kalluvalappil Gangadharan

[1]*Department of Mechanical Engineering, National Institute of Technology Karnataka, P.O. Shrinivasnagar, Surathkal, Mangaluru, India-575025*

*Received 28 April 2022, Accepted 21 December 2022*

## ABSTRACT

*In the present scenario, automobile sector has witnessed ample amount research and development to provide a greater comfort zone to the passenger. The term 'comfort' includes not only economical meaning but also a pleasant feeling through the journey by mitigating road disturbances reaching the passenger. In the present work, an effort has been dedicated to design, fabricate and characterize a magneto-rheological (MR) damper suitable for automobile application. MR damper is filled with magneto-rheological fluid the attribute of which can be quickly deviated with variation in externally applied magnetic field. Damper characterization has been performed for different amplitudes, frequencies and currents. These rheological results have been used to mathematically model the damper characteristics. Later, using the mathematical model, an attempt has been made to analyze the dynamic mannerism of the MR damper in a quarter car simulation model. For the given road input, the suspension system with MR damper has shown its ability in suppressing the road disturbance in a greater manner.*

*Keywords: MR damper, shear mode, characterization, quarter car.*

## INTRODUCTION

Smart materials are those which act in a special manner when subjected to external changes. Several studies are being conducted on these kinds of materials due to their advanced behavior and considering their probable potential use in future science. One among these smart materials is magneto-rheological (MR) fluid, which was first reported by Rabinow in 1948 in the application of magneto-rheological clutch [1]. Main constituents of MR fluid are ferrous particle, a base fluid and additives added for stability. Many combinations of these three constituents have been studied and reported in past research works [2, 3]. Due to the lightning variable response of MR fluid, it is being used in the applications such as MR clutch, MR damper, MR brakes, etc. [3, 4].

Goldasz presented and analyzed the concept of twin tube magneto-rheological damper considering certain nonlinear properties of fluid [4]. The

**Correspondence to: N P Puneet, Department of Mechanical Engineering, National Institute of Technology Karnataka, P.O. Shrinivasnagar, Surathkal, Mangaluru, India- 575025, E-mail: puneetnp12@gmail.com.*

results were analyzed by changing the design variables. Zhu et al. presented a review on magneto-rheological dampers for different applications developed by various researchers and concluded with some salient observations from different dampers and their designs [5]. Nguyen and Choi demonstrated an optimal design for magneto-rheological damper with the help of finite element analysis [6]. Geometric design optimization was carried out mainly considering damping force and dynamic range. MR damper suitable for certain automobile front suspension was designed and characterized by Tu et al. and later, the characteristic curve fitting was done using Bingham model [7]. Gurubasavaraju et al. tried to optimize parameters like fluid gap, iron particle percentage and the current supply to enhance damping effect of MR damper using particle swarm optimization technique [8]. Response surface methodology was also adopted to understand the effect of influencing factors. An approach using design of experiment was used by Shivaram and Gangadharan to model the MR damper behavior and response surface plots were shown [9]. Desai et al. designed, fabricated as well as characterized a double tube magneto-rheological damper which is suitable for suspension system of a passenger van [10]. Valve mode was considered in designing the MR damper and Bouc-Wen theory was applied to model the hysteresis nature of damper. MR damper for the purpose of earthquake mitigation was designed, tested and analyzed by Xu et al. [11]. Also, experimental and numerical results were compared with a proposed mathematical method. Influence of various material qualities on the magnetic flux density in the annular flow region was investigated by Gurubasavaraju et al. [12]. Optimization of design variables was also executed to generate higher flux density in the fluid flow region. Chooi and Oyadiji developed mathematical model for flow behavior of MR fluid via annular gap of damper and claimed credibility of model to describe non linear, hysteretic and asymmetric behavior of MR damper [13].

In this work, an effort has been put to design, fabricate and characterize MR damper suitable for vehicle application. For the characterization of damper, the fluid has been prepared in the laboratory to check the damping ability of the fluid. The characterization results have been used as mathematical model which have been implemented in quarter car simulation.

## Geometric design of magneto-rheological (MR) damper

Design of MR damper is basically dependent of the dynamic range which can be stated as the ratio of 'controllable force' (C.F.) to the 'uncontrollable force' (U.F.). The entire damping force of the MR damper is depending on three kinds of forces: force because of viscosity ($F_\eta$), force as a result of field induced shear ($F_\tau$) and frictional force ($F_f$). Hence, the dynamic range (DR) can be defined as:

$$DR = \frac{C.F}{U.F} = \frac{F_\tau}{F_\eta + F_f} \tag{1}$$

In this present work, the design of MR damper has been made on the basis of dynamic range and maximum damping force expected [11]. According to Bingham model, the plastic viscous force ($F_\eta$) and field induced shear force ($F_\tau$) can be written as:

$$F_\eta = \left(1 + \frac{whV}{2Q}\right)\frac{12\eta Q L A_p}{wh^3} \tag{2}$$

$$F_\tau = \left(2.07 + \frac{12Q\eta}{12Q\eta + 0.4wh^2\tau_y}\right)\frac{\tau_y p A_p}{h} sgn(V) \tag{3}$$

where: $Q$ is the volumetric flow rate, $A_p$ is the effective area of the piston ($A_p = \pi(d_p^2 - d^2)/4$), $d$ is the piston rod diameter, $p$ is the pole length, $w$ is the mean circumference of the annular flow path ($w = \pi(d_p + g)$), $L$ is the total axial pole length ($L = m + p$), $d_p$ is the piston head diameter, $V$ is the relative velocity between cylinder and the

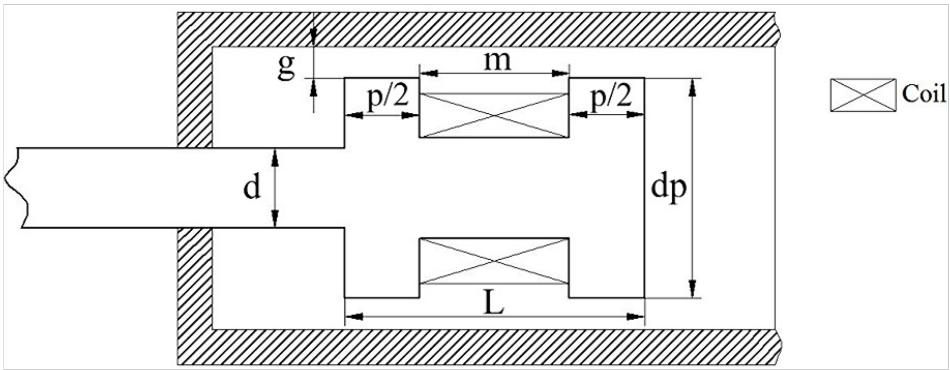


Fig. 1. Geometric nomenclature of MR damper piston.

Table 1. Optimized dimensions of MR damper piston.

| Sl. No. | Design variable | Optimized dimension (mm) |
|---|---|---|
| 1 | Diameter of Piston head ($d_p$) | 24.92 ≓ 25 |
| 2 | Piston rod diameter ($d$) | 10 |
| 3 | Pole length ($p$) | 4 |
| 4 | Total axial pole length ($L$) | 29.91 ≓ 30 |
| 5 | Annular flow path gap ($g$) | 0.69 ≓ 0.7 |

piston, $\eta$ is the apparent viscosity of MR fluid in the absence of magnetic field, $\tau_y$ is the yield shear strength of fluid and $g$ is the annular fluid flow gap. The geometric nomenclature is as shown in Fig. 1.

For a damper to be designed, it is always necessary to keep both dynamic range and the damping force as high as possible or for an expected level. Hence, to find the essential dimensions of the piston, the problem boundary is considered as optimization problem.

The optimization of the dimensions is subjected to achieving maximum damping force of 2 kN with a dynamic range of 3 and with an operating velocity of 0.2 ms$^{-1}$. The design variables accounted were piston head diameter ($d_p$), diameter of piston rod ($d$), pole length ($p$), total length of axial pole ($L$) and annular flow gap ($g$). The mentioned design variables were to be optimized with above mentioned conditions. Along with this, for achieving better design, the fluid property of commercially existing MR fluid 132 DG (from Lord Corporation), has been considering during design phase. Achievement of dynamic range was considered as objective function along with a constraint of maximum damping force. The MATLAB function was used to reach the objective, with proper adjustment of design parameters (in this case, dimensions of piston). Optimized dimensions of the MR damper piston geometry is provided in Table 1.

The designed MR damper has been fabricated and is shown in Fig. 2. The outer cylinder of the

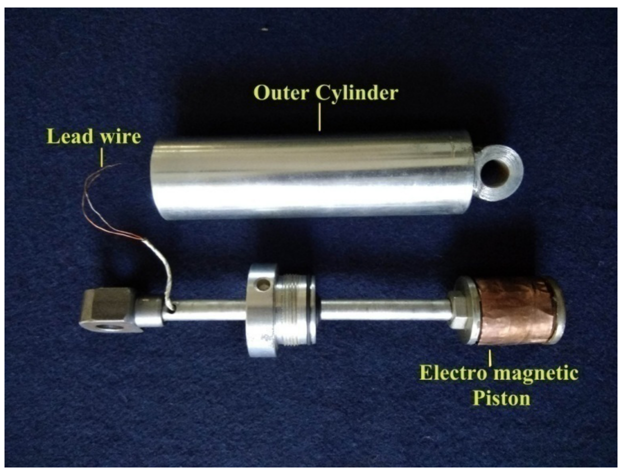


Fig. 2. Fabricated MR damper.

MR damper and the piston were fabricated using AISI 1018 steel which is having good magnetic permeability.

## EXPERIMENTAL

The damper characterization has been performed to understand the dynamic nature of MR damper by using force versus displacement data. The characterization tests were carried out in the dynamic testing machine (HEICO make). The damper testing machine (DTM) is capable of hydraulic actuation up to ± 20 kN force with 1.2 $ms^{-1}$ peak velocity and is powered by 3 phase motor. The machine comprises of linear position transducer for measuring the displacement and strain gauge based load cell for damper force measurement. The acquired information can be collected using data acquisition system (DAQ) which is in built with MOOG controller used for varying the input conditions. The damper testing machine is displayed in Fig. 3.

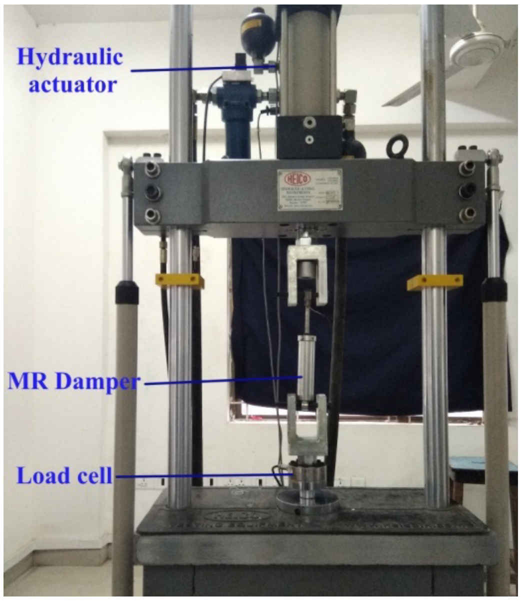


Fig. 3. Damper Testing Machine.

### Characterization of magneto-rheological damper

The dynamic performance of the designed MR damper is primarily understood with the force-displacement data obtained using characterization in damper testing machine. In this work, characterization of MR damper has been performed for different frequencies, amplitudes and currents supplied. The characterization has also been performed with no supply of current, as well. These conditions are listed in Table 2.

The MR fluid for this experimentation purpose was prepared in the laboratory, with 70 % weight fraction of electrolytic iron powder and remaining weight fraction of paraffin oil as base fluid. To avoid quick sedimentation of iron particles, a little amount of oleic acid was added as additive.

## RESULTS AND DISCUSSION

This section describes the force-displacement behaviour of MR damper when subjected to different amplitudes, frequencies and currents as detailed in Table 2. It is necessary to observe the differentiation of force behaviour with change in current supplied.

Fig. 4 describes the distinction in damping force achieved with variation in current for 5 mm amplitude test condition. From the figure, a clear distinguished behavior in force enhancement has been observed when tested without and with supply of current. With variation of current supplied, a significant amount of increase in damping force has been noted for the designed MR damper. Similar, nature of damping force has

Table 2. Conditions in damper characterization experiment.

| Sl. No. | Frequency of operation (Hz) | Amplitudes (mm) | Supplied Current (A) |
|---|---|---|---|
| 1 | 1.5 | 5 | 0.25 |
| 2 | 2 | 10 | 0.75 |
| 3 | 2.5 | 15 | 1.25 |

been observed for 10 mm and 15 mm amplitude test conditions. The maximum force achieved in each test condition has been listed in Table 3, where 'f' represents frequency of operation (Hz), 'A' represents displacement amplitude (mm), 'I' for current (A) and max force in kN.

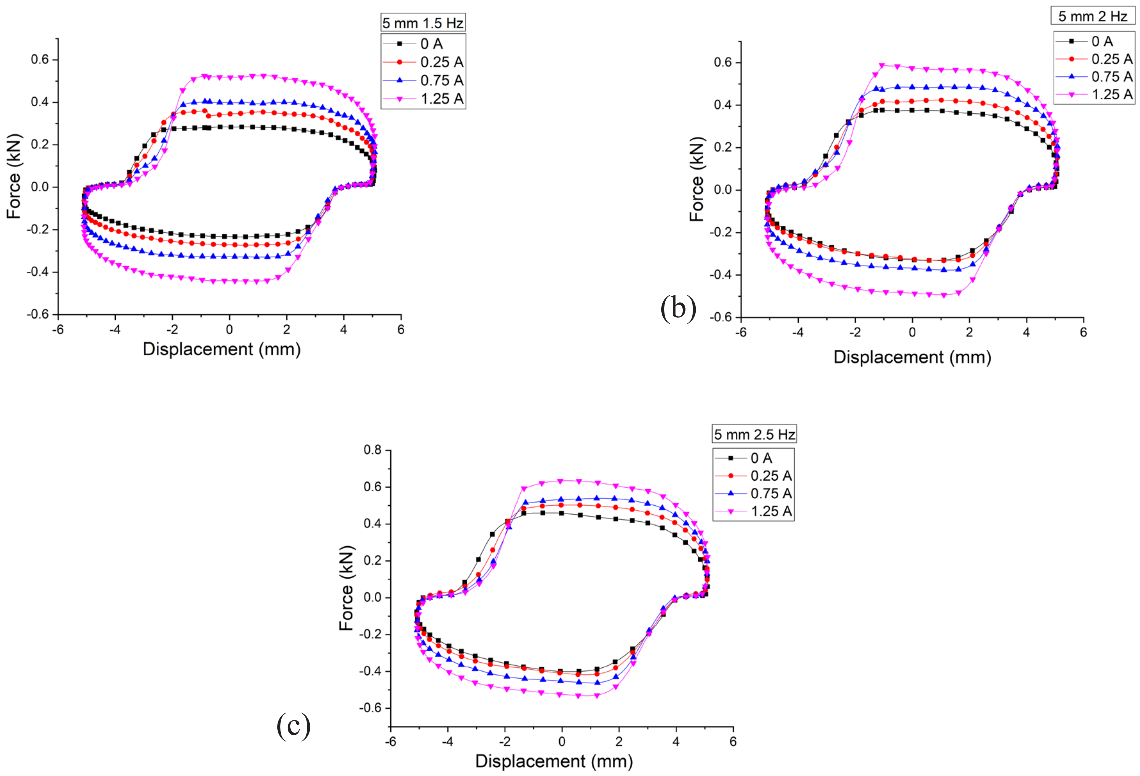


Fig. 4. Force-displacement curves with variation in current, for 5mm and (a) 1.5 Hz, (b) 2 Hz and (c) 2.5 Hz.

Table 3. Maximum force for different displacement amplitudes, frequencies and currents.

| f (Hz) | A (mm) | I (A) | Max Force (kN) | f (Hz) | A (mm) | I (A) | Max Force (kN) | f (Hz) | A (mm) | I (A) | Max Force (kN) |
|---|---|---|---|---|---|---|---|---|---|---|---|
| 1.5 | 5 | 0 | 0.2842 | 1.5 | 10 | 0 | 0.5127 | 1.5 | 15 | 0 | 0.87 |
| 1.5 | 5 | 0.25 | 0.3611 | 1.5 | 10 | 0.25 | 0.5275 | 1.5 | 15 | 0.25 | 0.9017 |
| 1.5 | 5 | 0.75 | 0.4066 | 1.5 | 10 | 0.75 | 0.6161 | 1.5 | 15 | 0.75 | 0.9554 |
| 1.5 | 5 | 1.25 | 0.526 | 1.5 | 10 | 1.25 | 0.6632 | 1.5 | 15 | 1.25 | 0.9579 |
| 2 | 5 | 0 | 0.385 | 2 | 10 | 0 | 0.6282 | 2 | 15 | 0 | 1.041 |
| 2 | 5 | 0.25 | 0.424 | 2 | 10 | 0.25 | 0.6324 | 2 | 15 | 0.25 | 1.0932 |
| 2 | 5 | 0.75 | 0.4869 | 2 | 10 | 0.75 | 0.7493 | 2 | 15 | 0.75 | 1.1139 |
| 2 | 5 | 1.25 | 0.5888 | 2 | 10 | 1.25 | 0.8057 | 2 | 15 | 1.25 | 1.1292 |
| 2.5 | 5 | 0 | 0.4604 | 2.5 | 10 | 0 | 0.7432 | 2.5 | 15 | 0 | 1.172 |
| 2.5 | 5 | 0.25 | 0.5027 | 2.5 | 10 | 0.25 | 0.7440 | 2.5 | 15 | 0.25 | 1.234 |
| 2.5 | 5 | 0.75 | 0.5391 | 2.5 | 10 | 0.75 | 0.8349 | 2.5 | 15 | 0.75 | 1.236 |
| 2.5 | 5 | 1.25 | 0.6351 | 2.5 | 10 | 1.25 | 0.9121 | 2.5 | 15 | 1.25 | 1.254 |

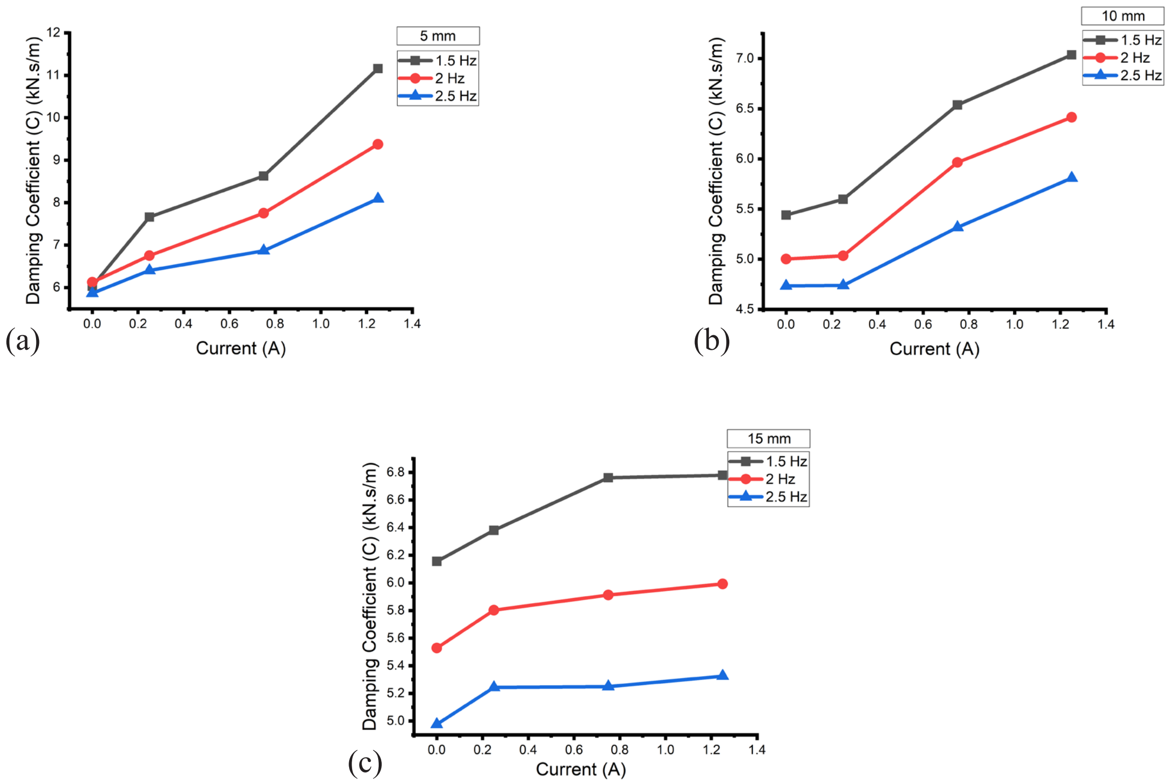


Fig. 5. Variation of damping coefficient with variation in current, for (a) 5mm, (b) 10mm and (c) 15mm.

A maximum damping force of 1.254 kN has been achieved form the designed damper at 15 mm amplitude, 2.5 Hz and 1.25 A current supplied. Hence, it is evident from the characteristic curves that there is a direct correlation between damping coefficients and the current supplied to MR damper. But for each set of amplitude and frequency, the characteristic equation may be different. Hence, for each case of frequency and amplitude, damping coefficient has been found out based on relation between damping force and velocity.

The relation between damping coefficient and current supplied to MR damper has been plotted in Fig. 5 for each case of amplitude. After knowing the damping coefficient value for each case, it is easy to find the correlation between damping coefficient and current supplied. This is done by using curve fitting method for each characteristic curve.

Table 4 provides the curve fitting equations for each set of combination of frequency and amplitude, which relates damping coefficients (C) with current supplied (I).

These correlations have been found out with an intension to find the MR damper performance when applied in quarter car simulation.

## Quarter car simulation

Quarter car is one of the simpler and efficient models which is used in the preliminary stage to check the performance of any designed parameter. In this work, the normal damper in the quarter car suspension has been replaced with MR damper for variable damping. A scheme of quarter car is shown in Fig. 6.

The equation of motion for the quarter car by considering tire stiffness and tire damping too, can be written in accordance with Newton's second law of motion and can be mathematically represented as:

Table 4. Equations relating damping coefficients and currents.

| Frequency (Hz) | Amplitudes (mm) | Correlation equation in terms of current |
|---|---|---|
| 1.5 | 5 | $C = 7.396I^3 - 13.51I^2 + 9.434I + 6.033$ |
| 2 | 5 | $C = 1.512I^3 - 2.159I^2 + 2.933I + 6.129$ |
| 2.5 | 5 | $C = 2.519I^3 - 4.150I^2 + 3.030I + 5.866$ |
| 1.5 | 10 | $C = -2.044I^3 + 3.717I^2 - 0.174I + 5.440$ |
| 2 | 10 | $C = -2.613I^3 + 4.916I^2 - 0.931I + 5.001$ |
| 2.5 | 10 | $C = -1.354I^3 + 2.871I^2 - 0.614I + 4.734$ |
| 1.5 | 15 | $C = -0.429I^3 + 0.242I^2 + 0.866I + 6.156$ |
| 2 | 15 | $C = 0.888I^3 - 2.056I^2 + 1.554I + 5.528$ |
| 2.5 | 15 | $C = 1.236I^3 - 2.643I^2 + 1.651I + 4.976$ |

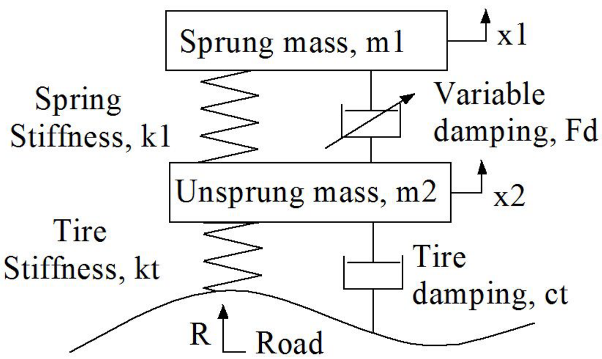

Fig. 6. Quarter car scheme.

Table 4. Quarter car parameters [14].

| Parameters | Values of parameters |
|---|---|
| Sprung mass, $m_1$ (kg) | 450 |
| Unsprung mass, $m_2$ (kg) | 50 |
| Spring stiffness of suspension, $k_1$ ($Nm^{-1}$) | 49000 |
| Tire stiffness, $k_t$ ($Nm^{-1}$) | 250000 |
| Tire damping coefficient, $c_t$ ($Nsm^{-1}$) | 1500 |

$$m_1\ddot{x}_1 + k_1(x_1 - x_2) + F_d = 0 \qquad (4)$$

$$m_2\ddot{x}_2 + c_t(\dot{x}_2 - \dot{R}) + k_t(x_2 - R) - \\ - k_1(x_1 - x_2) - F_d = 0 \qquad (5)$$

The parameters chosen for quarter car simulation have been listed in Table 5 [14].

Using the correlation equations as listed in Table 4, the damping in the suspension has been varied in the MATLAB/Simulink model for each case of dynamic condition. For the simulation purpose, the quarter car has been run over a sine wave profile (as road) which has 10 cm amplitude and 12 m wavelength. The quarter car has been moved with the velocity of 20 $ms^{-1}$.

**Results of quarter car simulation**

The variation in root-mean-square (RMS) acceleration of the sprung mass (in $ms^{-2}$) with variation in current for each dynamic condition has been plotted in Fig. 7.

It is evident from the plots shown in Fig. 7 that, there is a decrement nature in RMS acceleration of sprung mass with hike in the current provision to the MR damper. Reduction in amplitude of RMS acceleration of sprung mass always provides a comfort feeling to the passenger. Therefore, the semi active MR damper is always helpful to provide better suspension feeling when compared to the normal passive damper.

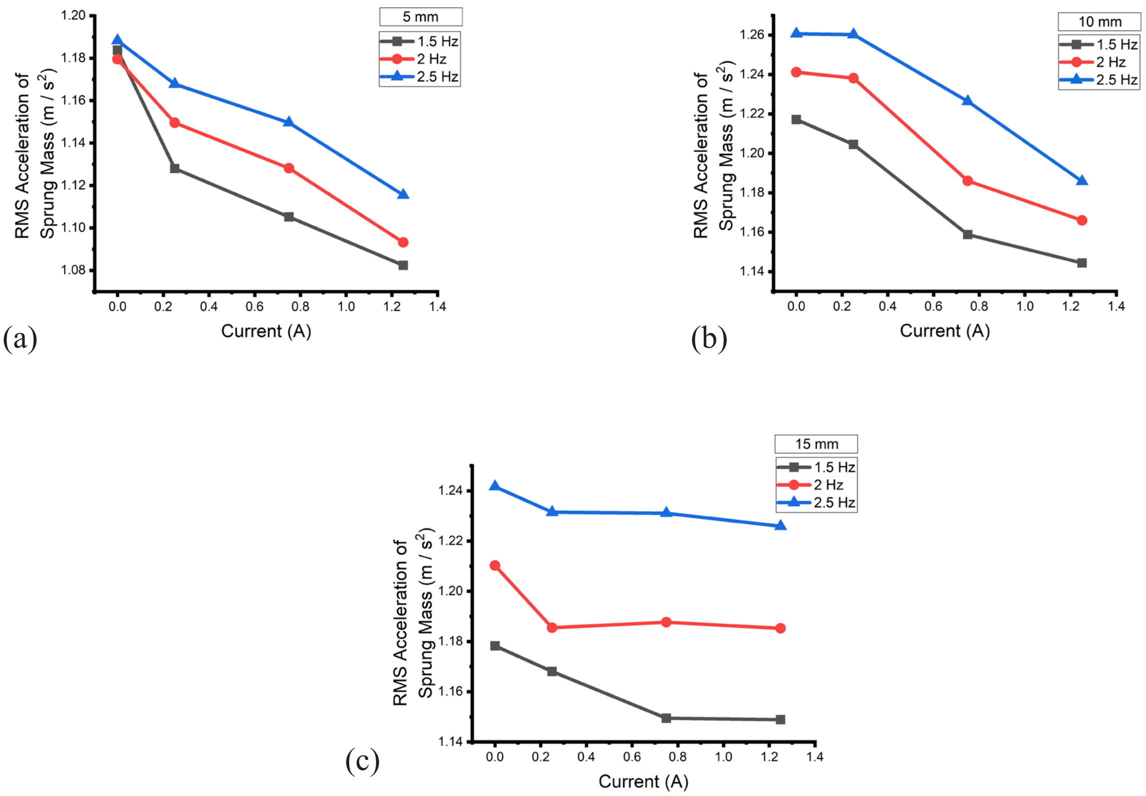


Fig. 7. RMS acceleration variation with variation in current, for (a) 5mm, (b) 10 mm and (c) 15 mm.

**CONCLUSIONS**

The present work emphasizes on the design, development and characterization experiments of MR damper preferably suitable for vehicle application. Initially the magneto-rheological damper was designed according to the Bingham model for shear and viscous forces. The objectives such as dynamic range and maximum damping force could able to provide the optimized piston dimensions of the MR damper. Using these optimized dimensions, the MR damper was fabricated and was tested using the damper testing machine. In this work, the MR fluid which was prepared in laboratory was used for experimentation. The characterization testing was able to provide the dynamic nature of MR damper in terms of force-displacement data. A maximum damping force of 1.254 kN was achieved for 2.5 Hz operating frequency and 15 mm displacement amplitude. To understand the damping capacity and feasibility of fabricated MR damper in vehicle application, the damper was used in the quarter car simulation model in MATLAB. The variable damping of the MR damper was provided to quarter car model in terms of mathematical relationship between damping coefficient and current supplied. The simulation results showed that the magnitude of RMS acceleration of sprung mass (which is a measuring parameter of comfort of passenger) was reduced with hike in current supply and hence showing the advantage of semi active system over passive system in vehicle suspension.

***Acknowledgements***

*The authors are grateful to "IMPRINT" project No. IMPRINT/2016/7330 entitled with "Development of Cost Effective Magneto-Rheological (MR) Fluid Damper in Two wheelers and Four Wheelers Automobile to Improve Ride Comfort and Stability" funded by the Ministry of Human Resource Development (MHRD) and the Ministry of Road Transport and Highways (MoRTH), Govt. of India.*

**REFERENCES**

1. J. Rabinow, The magnetic fluid clutch, AIEE. Transact., 67, 1948, 1308-1315.
2. A.A. Alghamdi, R. Lostado, A.G. Olabi, Magneto-Rheological Fluid Technology, In: J.P.Davim (Ed.), Modern Mechanical Engineering, Springer Press, Berlin, Heidelberg, 2014, p. 43-62.
3. M. Ashtiani, S.H. Hashemabadi, A. Ghaffari, A review on the magnetorheological fluid preparation and stabilization, J. Magn. Magn. Mater, 374, 2015, 716-730.
4. J. Gołdasz, Theoretical study of a twin-tube magnetorheological damper concept, J. Theor. Appl. Mech., 53, (4), 2015, 885-894.
5. X. Zhu, X. Jing, L. Cheng, Magnetorheological fluid dampers: a review on structure design and analysis, J. Intell. Mater. Syst.Struct., 23, (8), 2012, 839-873.
6. Q.H. Nguyen, S.B. Choi, Optimal design of a vehicle magnetorheological damper considering the damping force and dynamic range, Smart Mater. Struct., 18, (1), 2008, 015013.
7. F. Tu, Q. Yang, C. He, L. Wang, Experimental study and design on automobile suspension made of magneto-rheological damper, Energy Procedia, 16, 2012, 417-425.
8. T.M. Gurubasavaraju, H. Kumar, M. Arun, Evaluation of optimal parameters of MR fluids for damper application using particle swarm and response surface optimization, J. Braz. Soc. Mech. Sci., 39, (9), 2017, 3683-3694.
9. A.C. Shivaram, K.V. Gangadharan, Statistical modeling of a magneto-rheological fluid damper using the design of experiments approach, Smart Mater. Struct.,16, (4), 2007, 1310.
10. R.M. Desai, M.E.H. Jamadar , H. Kumar, S. Joladarashi, S.C. Rajasekaran, Design and experimental characterization of a twin-tube MR damper for a passenger van, J. Braz. Soc. Mech. Sci., 41, (8), 2019, 1-21.
11. Z.D. Xu, L.F. Sha, X. Zhang, H.H. Ye, Design, performance test and analysis on magnetorheological damper for earthquake mitigation, Struct. Control. Health. Monit., 20, (6), 2013, 956-970.
12. T.M. Gurubasavaraju, H. Kumar, M. Arun, Optimisation of monotube magnetorheological damper under shear mode, J. Braz. Soc. Mech. Sci., 39, (6), 2017, 2225-2240.
13. W.W. Chooi, S.O. Oyadiji, Mathematical modeling, analysis, and design of magnetorheological (MR) dampers, J. Vib. Acoust., 131, (6), 2009, 061002.
14. Gurubasavaraju, H. Kumar, M. Arun, Effect of rheological properties of MR fluid on dynamic performance of semiactive suspension with MR damper, Proceedings of 13th International Conference on Vibration Problems, IIT Guwahati, India, 2017, 1-9.